ORIGINAL ARTICLE

Highly Selective and Sensitive Colorimetric and Fluorescent Chemosensors for Rapid Detection of Cyanide Anions in Aqueous Medium: Investigation on Supramolecular Recognition of Tweezer-shaped Salophenes

Hossein Reza Darabi[1] · Ramo Nazarian[1] · Sepideh Alizadeh[1] · Kioumars Aghapoor[1] · Leila Ebadinia[1]

Abstract

Three tweezer-shaped salophenes having catechols (**1**), phenols (**2**) and anisoles (**3**) units in conjunction to the dipodal Schiff bases have been applied for the optical sensing of cyanide (CN^-) ions in CH_3CN-H_2O (7:3) as solvent of choice. Among them, compounds **1** and **2** recognized CN^-, relying on distinct color and spectral changes. They are easy-to-use probes that exhibit extremely high sensitivity (limit of detection = 1–10 nM), rapid response (5 s) and excellent selectivity. Moreover, the visual detection and concentration determination of CN^- by solution test kits of both sensors are the advantages for the practical applications. Based on the fluorescence and NMR spectroscopy, as well as the OH^- and reversibility experiments, the explicit effect of hydroxyl groups on sensing and as well the different recognition of **1** and **2** toward CN^- ions was proved. While probe **1** senses CN^- via deprotonation, probe **2** recognizes it through an intramolecular aldimine condensation cyclization, leading to formation of anions of dihydroxyquinoxaline **4**. This chemodosimetry is being reported for the first time in a Schiff's base. Furthermore, the similarity of fluorescence and NMR responses of **2** and **4** toward CN^- supports the proposed process.

Keywords Salophenes · Schiff base · Cyanide sensing · IACC process · Test kits

Introduction

Supramolecular chemistry is a relatively young area of interdisciplinary field of science in which the design of receptors is a main principle for making nonbonding supramolecular interactions with substrates. In order to produce high levels of affinity and selectivity, the binding ability of receptors is related to mutual size, shape, rigidity and binding sites with analytes [1, 2].

The inevitable widespread use of cyanide ion (CN^-) in various modern industries, such as the polymer industry and gold extraction process, has polluted water resources [3–5]. Given that CN^- has the capability to suppress the transportation process of oxygen in human body, the concentration control of CN^- in various sources of water, under the WHO allowable level, is an important duty [6]. Therefore, the development of new optical chemosensors for this hypertoxic ion is a paramount challenge.

Although there are numerous efficient optical chemosensors to recognize CN^- in various samples, the design of an accurate, cost-effective, easily synthesized and fast-response sensor for on-site CN^- detection is still urgently needed [7–9]. Therefore, the monitoring of remote polluted sites can be easily achieved by portable sensitive and selective optical sensors in countering environmental crisis.

Schiff bases, shown as **S1**-**S13** in Table 1, have been recently applied as optical chemosensors for the detection of CN^-. As clear in their structures, the imine groups are located at the ortho position of the hydroxyl groups with a possible intramolecular hydrogen bonds (O-H...N = C) [10]. According to the intrinsic nature of CN^-, both imine and hydroxyl groups of these Schiff bases are important binding site for CN^- recognition. In this regard, the imine groups in the structures of **S1**-**S8** have been activated through the resonance-assisted hydrogen bonds to promote the

✉ Hossein Reza Darabi
darabi@ccerci.ac.ir; r_darabi@yahoo.com

1 Nano & Organic Synthesis Laboratory, Chemistry & Chemical Engineering Research Center of Iran, Pajoohesh Blvd., km 17, Karaj Hwy, 14968-13151 Tehran, Iran

nucleophilic addition of CN⁻ on imine groups [11–17]. In contrast, CN⁻ sensing of **S9**-**S13** is taken place via the deprotonation of hydroxyl groups in which imines are remained inert [18–22].

The supramolecular recognition of salophenes **1**–**3** and their analogues for coordination with various metal ions have been already investigated [23–28]. However, there is no report on evaluation of these dipodal Schiff bases for sensing of CN⁻, whileas they have suitable coordinating sites like imine and hydroxyl moeities in their tweezer-shaped architecture (Scheme 1).

Among probes **S1**-**S13** listed in Table 1, the dipodal probes **S7**-**S9** have the closest architecture to **1**–**3**. While **S7** and **S8** undergo deprotonation followed by nucleophilic attack of CN⁻ to imine bond via Strecker's reaction mechanism, [17] the CN⁻ sensing of **S9** is taken place via deprotonation followed by disaggregation [18].

For a long time, we have been interested to the design and synthesis of various supramolecular based chemosensors [29–40]. In this regards, we have designed and synthesized some optical receptors for sensing of CN⁻ which are based on the different recognition mechanism, such as deprotonation, [37, 38] metal-replacement [39] and aggregation induced emission [40].

We herein report the CN⁻ sensing of salophenes **1**–**3** by optical methods. Among them, compounds **1** and **2** recognized CN⁻ which bolded the critical role of hydroxyl groups. Both sensors are applicable in buffer solutions and show highly selectivity, very low detection limit (1–10 nM) and rapid response toward CN⁻. As for practical applications, the solution test kits of both probes was successful for quantitative measurment of CN⁻. Moreover, the various experimental data

propose that the sensing mechanism of **1** and **2** is taken place in different ways.

Results and Discussion

The compounds **1** and **2** were simply synthesized by the condensation reaction of 1,2-diaminobenzene with 2,3-dihydroxy benzaldehyde, [23, 24] or 2-hydroxy benzaldehyde [25] respectively (Schemes S1 and S2). The known compound **4** has been also prepared from the reaction of NaCN with **2** for 48–64 h stirring at room temperature under harsh reaction condition [26–28]. The synthesis routes are drawn in Schemes S1-S3. All products were characterized by ^1H NMR measurements which are identical to those of the reported data (Figs. S1-S3).

Optical Response of 1 Toward CN⁻ Ion

To investigate the optical response of **1** to CN⁻ ion, a solution of NaCN was gradually added to $CH_3CN : H_2O$ buffered solution (7:3, pH 7.4) of **1** and after each addition the absorption and emission spectra were recorded.

The UV–vis spectra of **1** exhibits two absorption peaks at 290 and 321 nm which are assigned to the π–π^* and n–π^* transition of the C = C and C = N bonds. When CN⁻ (0–1.5 equiv.) is added into the buffer solution of **1**, the intensity of original peaks gradually reduced, whereas a new peak/ shoulder at 410 nm appeared (Fig. 1a). At the same time, a clear isosbestic point at 355 nm is formed to indicate a distinct interaction between **1** and CN⁻. This spectral change is supported by the color change of solutions from colorless to
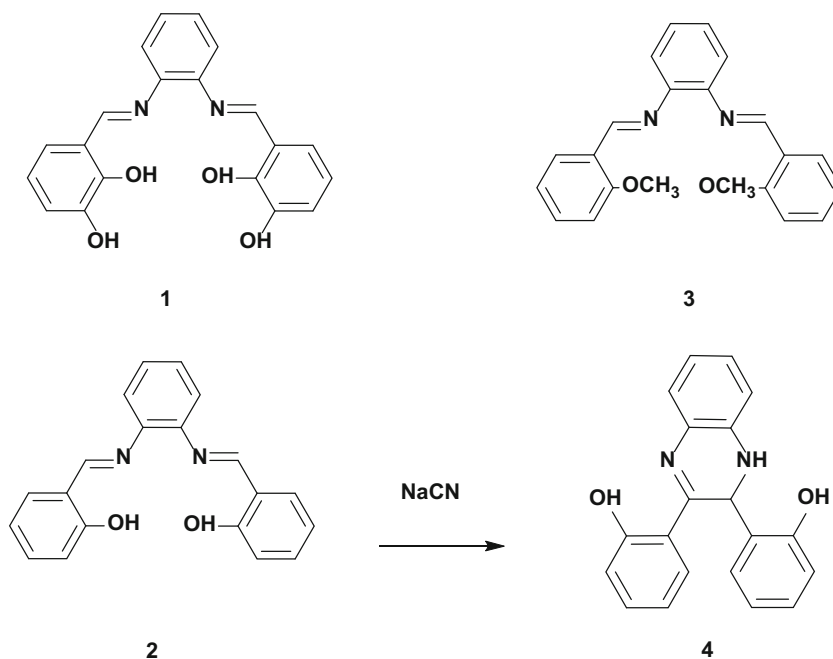
Scheme 1 Structure of compounds **1**–**4**

Table 1 Detection of CN⁻ by Schiff base probes S1-S13 (N.A.= Nucleophilic addition; D.P.= Deprotonation)

Probe	Substrate	Complex	Solvent system	Mechanism	Process	DL	Ref
S1			DMSO:H₂O	N.A.	Irreversible	14 pM	11
S2			DMSO:H₂O	N.A.	Irreversible	3.1 nM	12
S3			DMSO:H₂O	N.A.	Irreversible	35 μM	13
S4			DMSO:H₂O	N.A.	Irreversible	105 μM	14
S5			DMSO:H₂O	N.A.	Irreversible	77 nM	15
S6			CH₃CN:H₂O	N.A.	Irreversible	1.9 μM	16
S7			DMSO:H₂O	N.A.	Irreversible	3 μM	17
S8			DMSO:H₂O	D.P.	Irreversible	1.65 μM	17
S9			DMSO:H₂O	D.P.	Reversible	55 nM	18
S10			EtOH:H₂O	D.P.	Reversible	0.28 μM	19
S11			DMSO:H₂O	D.P.	Reversible	210 μM	20
S12			CH₃CN:H₂O	D.P.	Reversible	1.2 μM	21
S13			CH₃CN:H₂O	D.P.	Reversible	1.65 μM	22

yellow (the inset of Fig. 1a). Therefore, the observed bathochromic shift suggests that the transition of intramolecular charge transfer (ICT) band is occurred through the deprotonation of the chemosensor **1** by CN⁻ [19–21, 41].
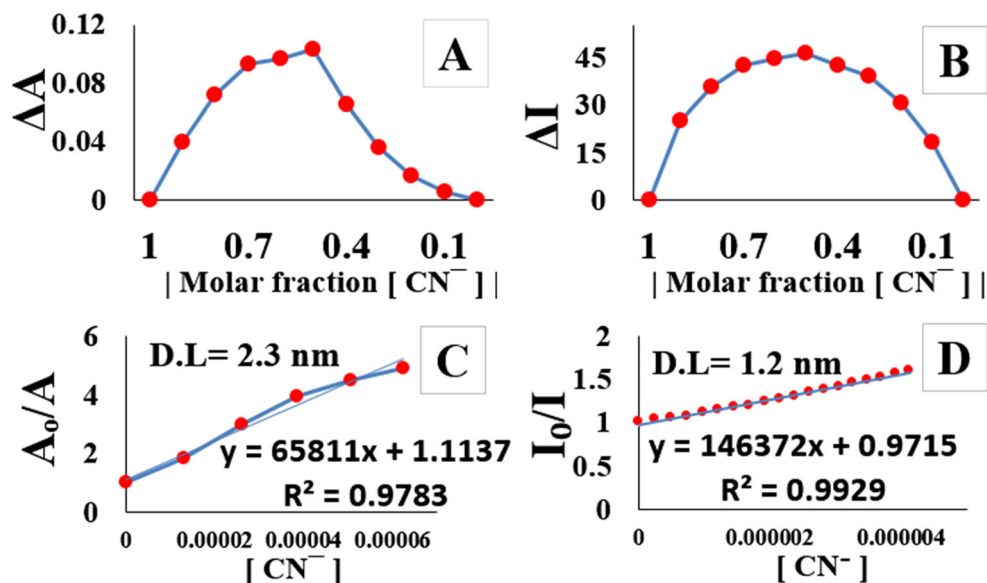
Fig. 1 **a** Absorbance and **b** emission spectra of **1** (0.015 μM) upon addition of CN⁻ ions (0–1.5 equiv.) in CH₃CN : H₂O buffered solution (7:3, pH 7.4)
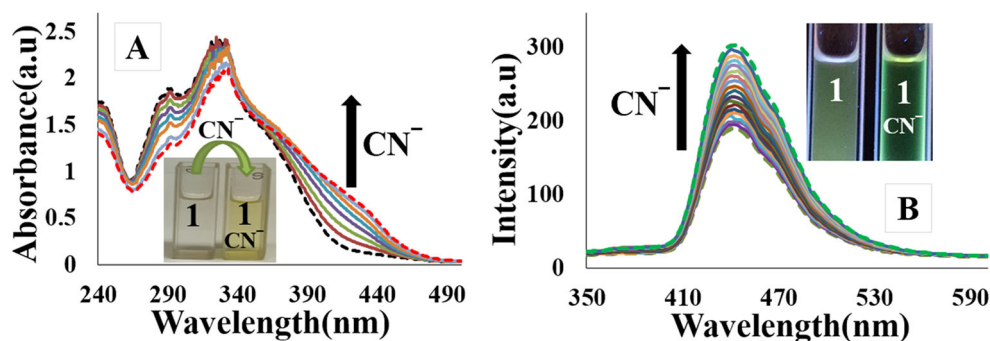
Compound **1** displays a single fluorescence emission band at 442 nm when excited at 400 nm. Upon the addition of CN⁻ (0–1.5 equiv.) to the solution of **1**, this emission peak is gradually increased with a virtually unchanged emission shift (Fig. 1b) and a more intensive green emission color which is perceptible to the naked eyes under 365 nm UV light (the inset of Fig. 1b). In contrast, other anions do not induce such changes (Fig. S4). The fluorescence enhancement might be attributed to the deprotonation of hydroxyl groups, through which an ICT process (from hydroxyl anion to the electron-deficient imine groups) can be improved [37].

The binding mode of **1** with CN⁻ was measured by Job plot analysis and gave a 1:1 stoichiometry (Fig. 2a and b). The optical response of **1** fits well with the Stern-Volmer equation to confirm the strong interaction between **1** and CN⁻ (Fig. 2c and d). The binding constants (K_a) were calculated using the Benesi-Hildebrand equation and found 2.8×10^3 and 1.0×10^5 M^{-1} by UV-vis and Fluorescence methods, respectively. According to calculations, a high sensitivity by fluorescence (LOD = 1.2 nM) and UV–vis (LOD = 2.3 nM) methods were obtained which are much lower than the maximum allowable level of CN⁻ ions in drinking water (1.9 μM) set by the WHO [6].

To evaluate the interference of CN⁻ with the following sodium anions (NO₂⁻, NO₃⁻, SCN⁻, HS⁻, S²⁻, Br⁻, Cl⁻, F⁻, I⁻, H₂PO₄⁻, IO₃⁻, IO₄⁻, ClO₄⁻, BrO₃⁻, ClO₃⁻, MoO₄²⁻, SO₃²⁻, S₂O₃²⁻, S₂O₄²⁻, S₂O₅²⁻, SO₄²⁻) competitive experiments by UV-vis (Fig. 3a) and fluorescence (Fig. 3b) spectroscopy were carried out and showed no interference between CN⁻ and other anions. Moreover, as the other anions, except CN⁻, did not induce the solution color change, the interference between CN⁻ and other anions is distinctable via solution color under naked eye (Fig. 3c and d). It means that among other anions, CN⁻ has the most basic and least hydrogen bonding character which might deprotonate the protons of catechol rings, resulting in the color change of solution [37, 38].

On the other hand, it was found that addition of different chloride cations (Li⁺, Na⁺, Ca²⁺, Ba²⁺, Sr²⁺, K⁺, Mg²⁺, Al³⁺, Cu²⁺, Cd²⁺, Co²⁺, Fe³⁺, Ni²⁺, Hg²⁺, Ag⁺, Mn²⁺, Pb²⁺, Zr⁴⁺) to solutions of **1** did not interfer the CN⁻ sensing (Fig. S5). The high selectivity of CN⁻ over cations confirmed that the deprotonation process is superior to metal complexation.

To figure out the interaction between **1** and CN⁻, ¹H NMR measurements were first performed in the presence of NaCN, as shown in Fig. 4a. When 1 equiv. of CN⁻ was added to the solutions of **1** in DMSO-d₆, the corresponding signals of the

Fig. 2 Job plots for the binding of **1** and CN⁻ based on absorbance (**a**) and emission (**b**) titrations. The changes in absorbance (**c**) and emission (**d**) intensity of **1** upon CN⁻ addition
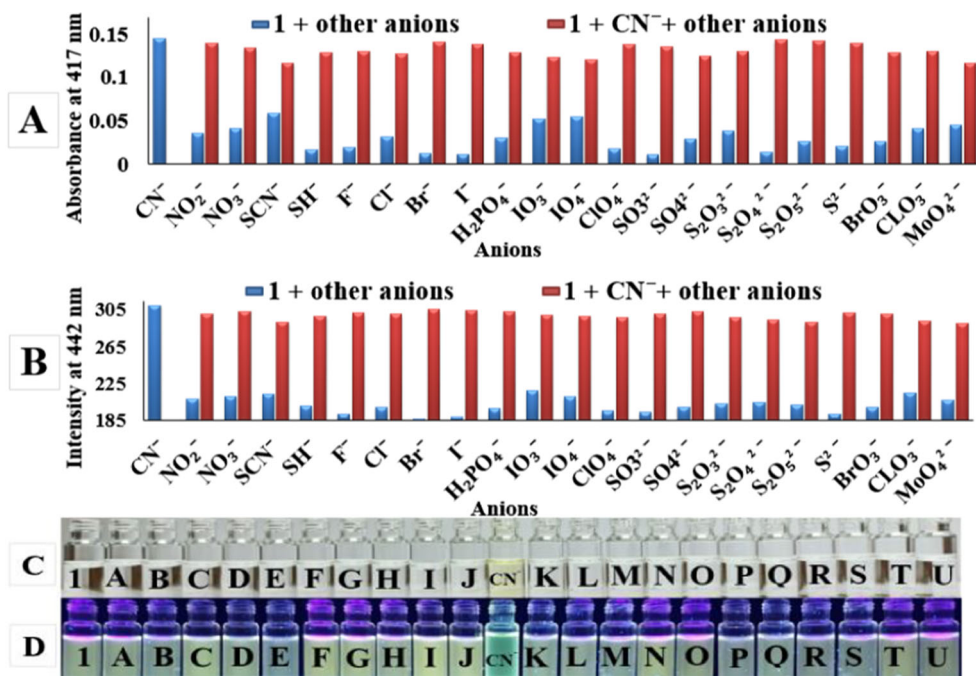
Fig. 3 Competition of CN⁻ with various anions under **a** UV-vis measurements and **b** fluorescence. **c** visual and **d** fluorescence images of **1** (1 equiv.) in the presence of 10 equiv. of various sodium anions CH₃CN : H₂O buffered solution (7:3, pH 7.4). (From A to U: F⁻, Cl⁻, Br⁻, I⁻, NO₂⁻, NO₃⁻, IO₃⁻, IO₄⁻, ClO₃⁻, ClO₄⁻, SCN⁻, CN⁻, H₂PO4⁻, S²⁻, SH⁻, SO₃⁻, SO₄²⁻, S₂O₃²⁻, S₂O₄²⁻, S₂O₅²⁻, BrO₃⁻, MoO₄²⁻)


OH protons at 10.5 and 13.5 ppm vanished, confirming the ¹H NMR result is consistent with the Job's plot result. At the same time, the imine peak shifted upfield slightly from 8.7 to 8.5 ppm to show that this functional group is inert to CN⁻ ions. Meanwhile, the peaks of aromatic rings showed upfield shield to different extent, indicating the increase of electron density through charge delocalization in the conjugated system [42]. In addition, no new peak related to formation of

Fig. 4 **a** ¹H NMR spectra of **1** in the presence of 1 equiv. of CN⁻. **b** and **c** The emission and absorption response of **1** to OH⁻ and CN⁻ ions in CH₃CN:H₂O (7:3)
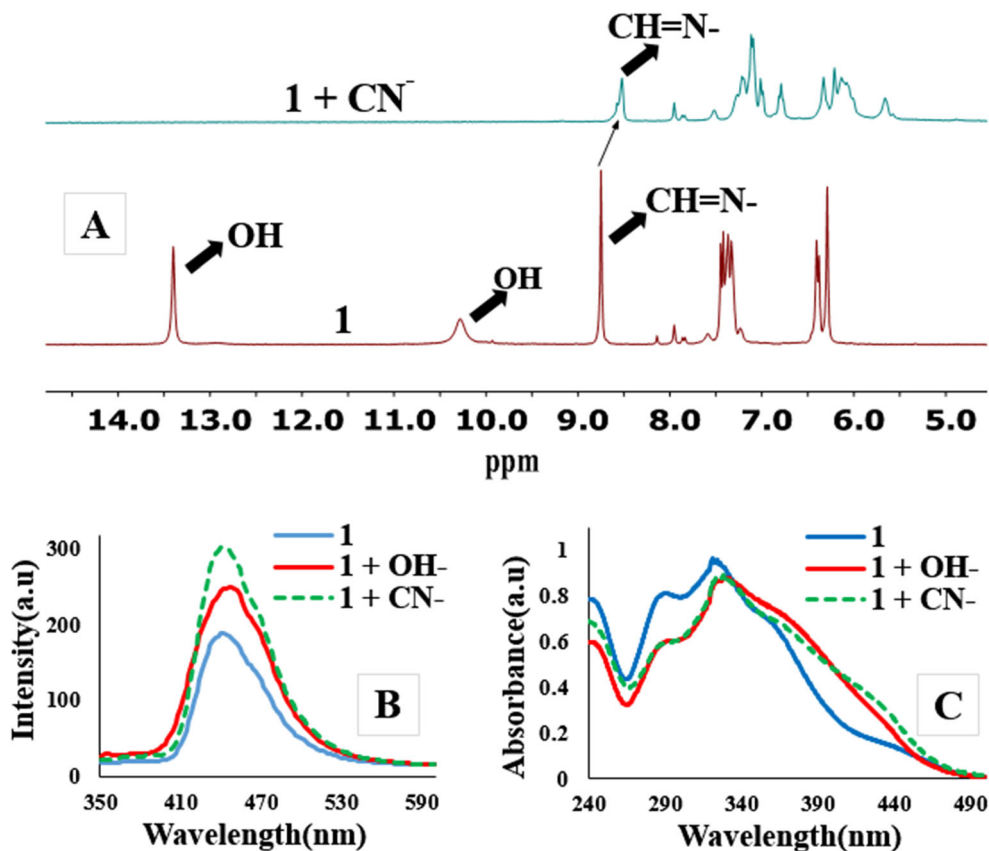
Scheme 2 Proposed recognition mechanism for sensor **1** and its reversibility route
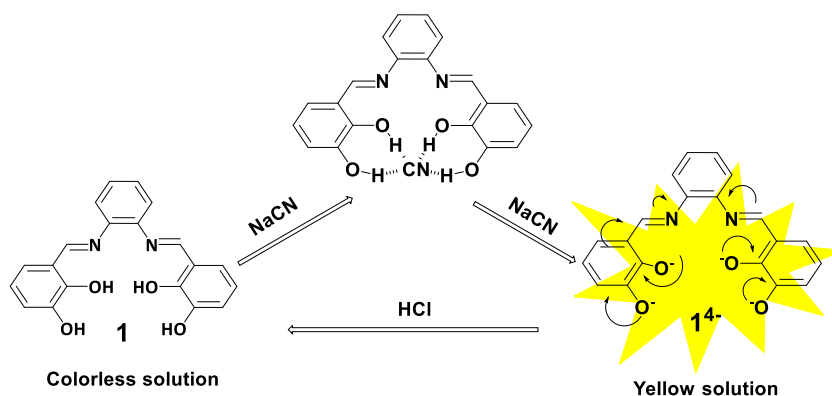
amine was observed to show that the nucleophilic addition of CN⁻ to the imine moiety did not occur.

To further support of CN⁻ sensing mechanism, the interaction between **1** and alkaline base (OH⁻) as a good blank sample for CN⁻ was investigated. As shown in Fig. 4b, c, the addition of OH⁻ or CN⁻ to **1** gave the identical emission and absorption spectrum to support the deprotonation mechanism of **1** [37, 38].

Based on the experimental data, **1** can recognize CN⁻ via its tetradentate site which formed between four hydroxyl groups. As depicted in Scheme 2, this binding site prohibits the nucleophilic attack of CN⁻ on imine groups.

Optical Response of 2 Toward CN⁻ Ion

The binding ability of **2** toward CN⁻ ions was also studied in $CH_3CN : H_2O$ buffered solution (7:3, pH 7.4) by UV–vis and fluorescence spectroscopy (Fig. 5).

The absorbance response of **2** to different amounts of CN⁻ are depicted in Fig. 5a. When 20 equiv. of CN⁻ was gradually added to **2**, the intensity of the absorption band at 320 nm decreases. At the same time, a new shoulder at 417 nm together with a clear isosbestic point at 370 nm was observed. These spectral changes is consistent with a distinct color change from colorless to pale yellow, as shown in Fig. 6c.

The fluorescence response of **2** to CN⁻ is more distinctable than its corresponding UV − vis spectrum. Upon addition of CN⁻ ions (0–30 equiv.) to a solution of **2** (0.015 μM), the

fluorescence peak at 466 nm was blue-shifted to 446 nm (Fig. 5b). This spectral changes is consistent with distinct color change of solution, as shown in inset of Fig. 5b. It is inferred that sensor **2** is converted to a new emissive product, shown as compound **4**, through which the electronic property has been changed. This change is evidenced by the non-linear emission response **2** to CN⁻, as shown in inset of Fig. 5b.

The binding mode of **2** with CN⁻ was measured by Job plot analysis and gave a 1:1 stoichiometry (Fig. S6). The calculated detection limit by fluorescence (2 μM) is remarkably lower than that of UV–vis (10 nM). However, using of emission intensity ratio (I_{466}/I_{446}) method improved the ratiometric detection of CN⁻ (0.9 μM, Fig. S7). In contrast, a linear response was observed in the 10–30 μM range and a detection limit as low as 8.2 nM was obtained.

To examine the selectivity, probe **2** was incubated with various anion species including (CN^-, NO_2^-, NO_3^-, SCN^-, HS^-, S^{2-}, Br^-, Cl^-, F^-, I^-, $H_2PO_4^-$, IO_3^-, IO_4^-, ClO_4^-, BrO_3^-, ClO_3^-, MoO_4^{2-}, SO_3^{2-}, $S_2O_3^{2-}$, $S_2O_4^{2-}$, $S_2O_5^{2-}$, SO_4^{2-}). Among them, only CN⁻ responded to **2** (Fig. 6a and b) with a distinct color and spectral change in solution (6 C, 6D and Fig. S8). We therefore assume CN⁻ selectivity of the dosimeter **2** over anions and cations (Fig. S9) is due to its unique reaction pathway, as shown in Scheme 3.

To investigate the reaction pathway of **2** with CN⁻, ¹H NMR measurement was carried out in DMSO-d₆ (Fig. 7a). When 1 equiv. of CN⁻ was added to solution of **2**, the protons of hydroxyls and imines at 13 and 8.9 ppm, respectively,

Fig. 5 Absorbance (**a**) and emission (**b**) spectra of **2** (0.015μM) upon addition of CN⁻ ions (0–30 equiv.) in $CH_3CN : H_2O$ buffered solution (7:3, pH 7.4)
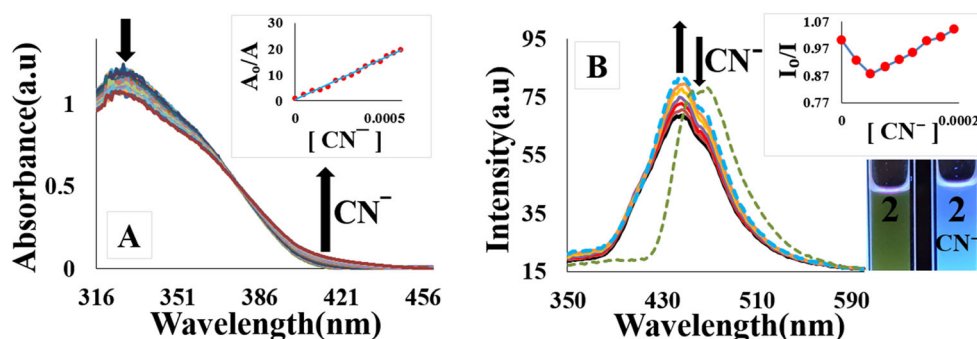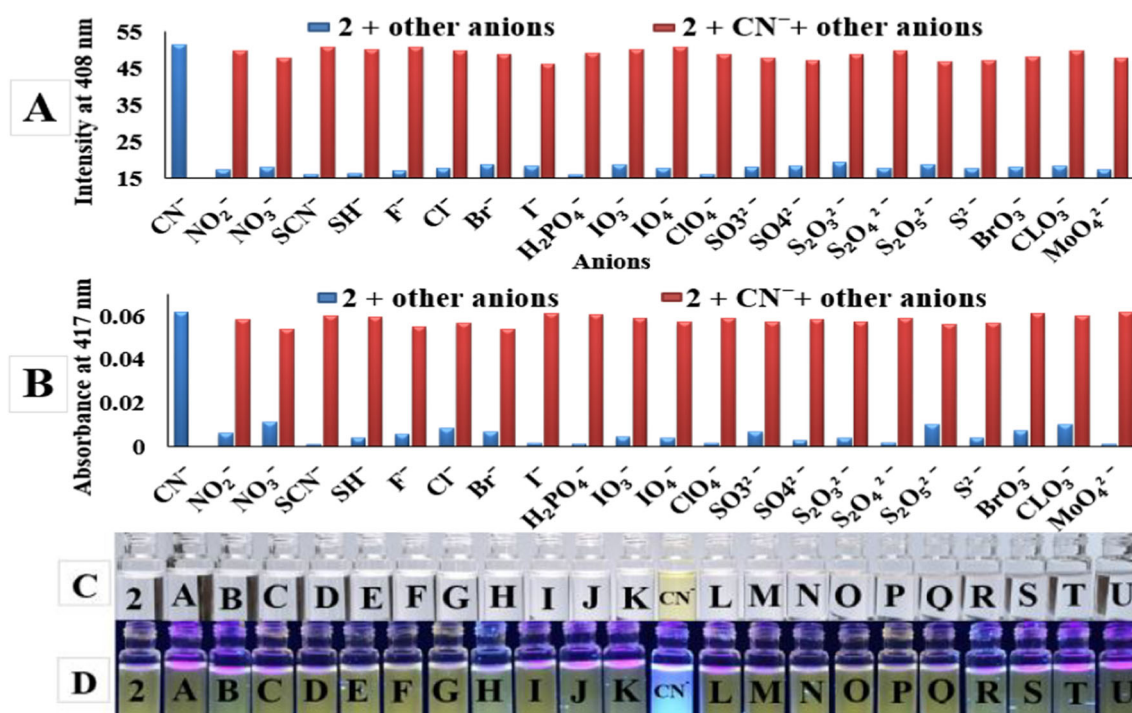
Fig. 6 Competition of CN⁻ with various anions under fluorescence (a) and UV-vis (b) measurements. Visual (c) and fluorescence (d) images of 2 (1 equiv.) in the presence of 10 equiv. of various sodium anions CH₃CN : H₂O buffered solution (7:3, pH 7.4). (From A to U: F⁻, Cl⁻, Br⁻, I⁻, NO₂⁻, NO₃⁻, IO₃⁻, IO₄⁻, ClO₃⁻, ClO₄⁻, SCN⁻, CN⁻, H₂PO4⁻, S²⁻, SH⁻, SO₃⁻, SO₄²⁻, S₂O₃²⁻, S₂O₄²⁻, S₂O₅²⁻, BrO₃⁻, MoO₄²⁻)

disappeared. Moreover, all the protons of aromatic rings exhibited an upfield shield on different levels. At the same time, a new broad peak at 4.5 ppm, related to the amine protons, appeared as attributed to the nucleophilic attack on imine moeities.

Furthermore, the interaction between 2 and CN⁻ was studied by the OH⁻ test. As shown in Fig. 7b, the emission peaks of 2 in the presence of CN⁻ and OH⁻ in CH₃CN:H₂O (7:3), unlike those of probe 1, are differ to each other. This difference is also observable by UV-vis spectroscopy Fig. 7c, with an improvement in MeOH:H₂O (7:3) to show that recognition mechanism of CN⁻ by 1 and 2 is taken place in different route.

As a result, NMR and OH⁻ data support the formation of a new compound 4 through the route depicted in Scheme 3.

Accordingly, an equivalent mixture of 2 and CN⁻ in MeOH was reacted at room temperature for 1 h and gave quantitative yield of dihydroxyquinoxaline 4. The structure of 4 was well supported by ¹H NMR and mass spectroscopy (Figs. S3 and S11) [26, 27]. As shown in Figs. 7 and 8, ¹H

NMR and fluorescence changes of 2 and 4 in the presence of CN⁻ is identical (Fig. 8b), confirming the CN⁻ sensing of 2 is happened via 4.

Compound 4 has two emission peaks at 470 and 520 nm (Fig. 9). Upon addition of CN⁻ (0–1.0 equiv.) to a solution of 4, the peak at 520 nm gradually disappeared. At the same time, the peak intensity at 470 nm was gradually increased. This unique feature can be attributed to gradual breaking of intramolecular hydrogen bonds of 4 followed by the deprotonation process. This response is fast and show highly sensitivity to CN⁻ (LOD = 6.5 nM) with significant color change from yellow to blue under 365 nm UV light (below inset of Fig. 9) with a binding constant of 5×10^3 M⁻¹ between 4 and CN⁻. On the other hand, UV-vis spectroscopy was not suitable method, because no absorption changes appeared when CN⁻ was added to 4 (Fig. S15).

Based on the mentioned spectral data, we depicted the sensing mechanism in Scheme 3. Therefore, CN⁻ attacks to the first aldimine group to form a cyano-adduct intermediate.

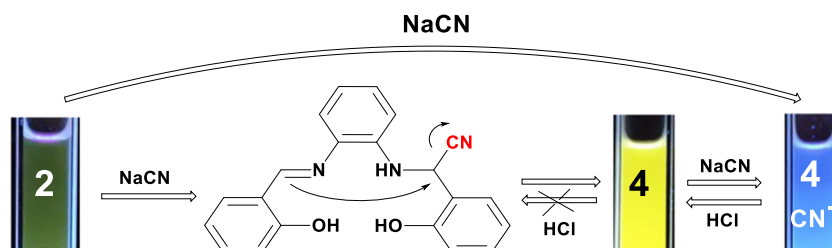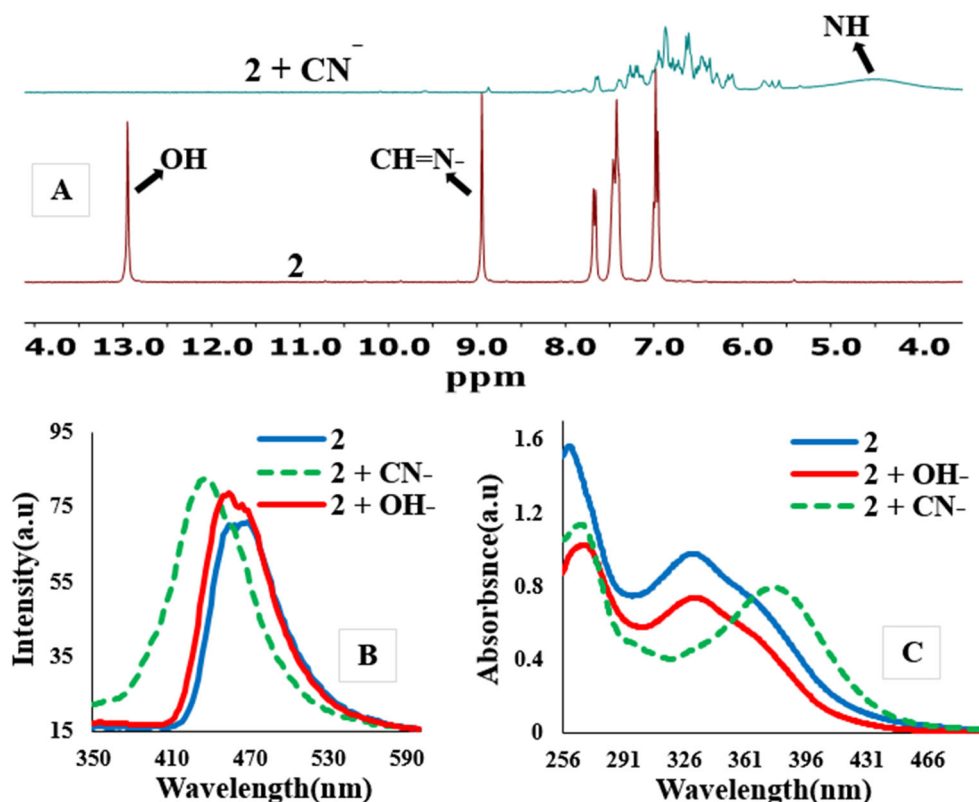Scheme 3 Proposed recognition mechanism for sensors 2 and 4 (the color changes are observable under UV light 365 nm)

The suitable distance between two aldimine groups of **2** promoted the intramolecular aldimine condensation cyclization (IACC) process on this intermediate, followed by formation of product **4**. On the other hand, The obtained spectral data by **4** in the presence of CN$^-$ is similar to those of **2** to confirm that the CN$^-$ sensing of **2** is occured via **4**.

Taking the structures of **2** and **3**, the comparison of their respective behavior to CN$^-$ may give clues about the proposed mechanism. In this regard, no obvious color and spectral changes for **3** was observed even in a large excess of CN$^-$. Therefore, the phenolic hydrogen may activate the imines groups of **2** through an intramolecular hydrogen bond [43].

Effect of Solvents on CN$^-$ Sensing

It is well known that solvents play a fundamental role in binding processes between host and guest [44]. In this study, to assess the impact of solvents on UV-vis and fluorescence spectroscopy of probes, CH3CN, MeOH and DMF together with their aqueous solutions were selected. As shown in Fig. S12, the absorption and emission spectroscopy of each compound, except absorption of **4**, is almost similar in all solvents. In contrast, the response of these compounds to CN$^-$ is solvent dependent, as shown in Table S1 and Figs. S13-S15. It was found that DMF solutions are not suitable solvents for
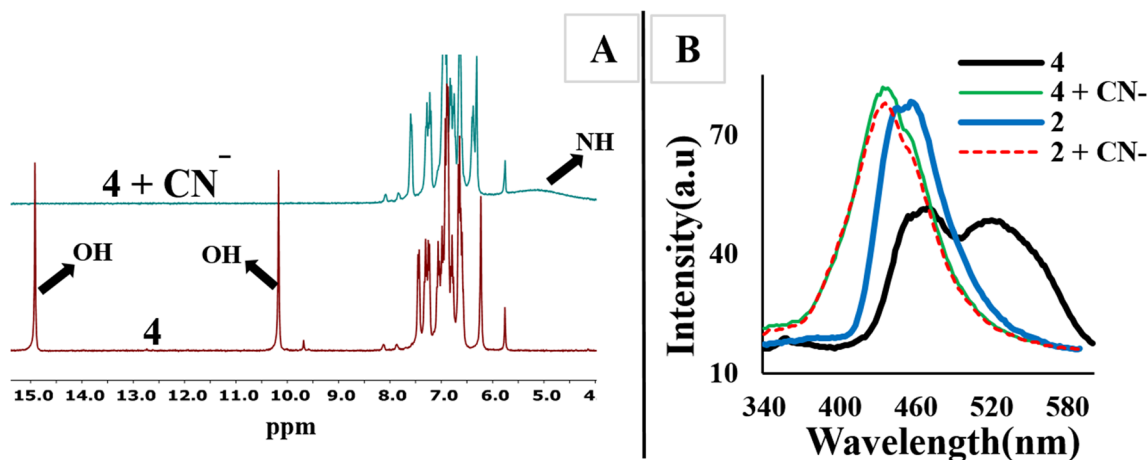

Fig. 8 **a** ^{1}H NMR of **4** in the presence of 1 equiv. of CN$^-$. **b** The comparison of fluorescence response of **2** and **4** to CN$^-$ ions
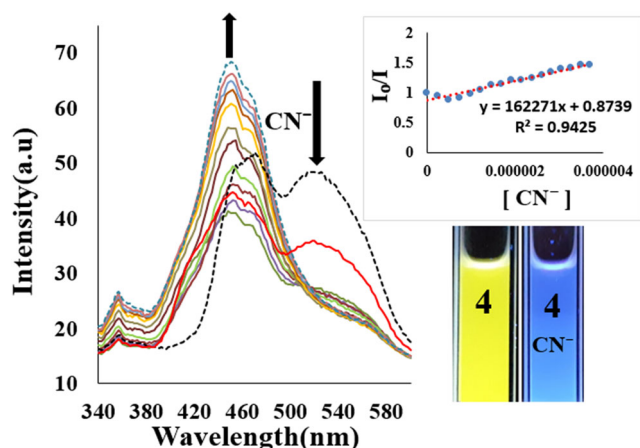
**Fig. 9** Emission spectra of **4** (0.1 μM) upon addition of CN⁻ ions (0–1 equiv.) in 30 % aqueous CH₃CN

CN⁻ sensing because of the insignificant spectral changes of probes. On the other hand, solutions of MeOH or CH₃CN bold the spectral response of probes in the presence of CN⁻. At the same time, the absorption and color response of MeOH solutions of **2** to CN⁻ becomes more outstanding which is suitable for quantitative experiments (see Figs. 7c and 12), whileas the calculated DLs for CN⁻ is above the level of WHO (2 μM as discussed in 2.4.3). Regarding the spectral response and DLs, therefore, CH₃CN : H₂O (7:3) is the solvent of choice for sensing tests of all probes. Notably, the addition of more amount of H₂O in CH₃CN led to decreased solubility of probes in solutions.

Practical Application

pH Dependence

Since the pH variation effects the charge distribution on a molecule, it can change the absorbance and fluorescence response of the probes. To check the versatility of probes **1** and **2** in different pH, the effects of pH on these probes and their complexes with CN⁻ by UV-vis and fluorescence spectroscopy were also studied. As shown in Fig. 10 and Fig. S10, the detection can work well in the pH range 5.0–8.0. Accordingly,
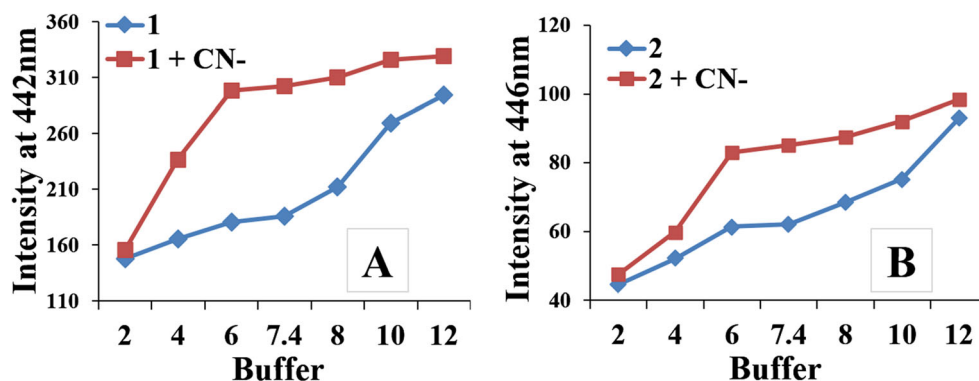
we set all measurements at buffer pH = 7.4 which is applicable for biological samples.

Reversibility Experiment

The reversibility between **1** and CN⁻ or **2** and CN⁻ were evaluated by the HCl addition experiments. When 1 equiv. of HCl was added to the mixture of **1** and CN⁻, the solution color changed from yellow to colorless (Fig. 11a). The color change was confirmed by the disappearance of the absorbance shoulder at 417 nm, suggesting the reversible deprotonation-protonation cycle after several cycles.

In contrast, probe **2** shows the irreversible behavior under the similar experiment to suggest a nucleophilic reaction was taken place on it.

The reversibility of probe **1** was also studied on silica gel plates. As shown in Fig. 11b, a colorless test strip was prepared by immersing TLC plate into MeOH solution of **1** (10⁻⁴ M). When this colorless paper was immersed into solution of CN⁻ (10⁻⁴ M), a yellow color appeared on it. This yellow color subsequently returned back to original color of **1** when plate immersed into solution of HCl (10⁻⁴ M). These results showed that sensor **1** can work well in both solution and solid state as portable kits for CN⁻ analysis.

Solution Kit Tests

The performance of **1** and **2** for qualitative detection of CN⁻ was evaluated. As shown in Fig. 12, the gradual color change from colorless to yellow with the addition of various concentrations of CN⁻ was detectable by both probes.

The visual color changes are accompanied with gradual increasing of absorption shoulder/peak of **1** in 30 % aqueous CH₃CN (Fig. 12a and c). In contrast, the observation of gradual color change of **2** in 30 % aqueous CH₃CN was almost impossible. Therefore, the measurements were carried out in 30 % aqueous MeOH which showed an improvement in gradual color and spectral changes (Fig. 12b and d). Although aqueous MeOH is suitable solvent for the qualitative study,

Fig. 10 The effect of pH on the emission of **1** (a) and **2** (b) with and without CN⁻ ions

Fig. 11 a Reversibility of **1** through UV-vis spectra and visual color change upon alternate addition of CN⁻ and HCl. **b** Photographs of **1** after the sequential immersion into water solution of CN⁻ and HCl on test strips under visible light
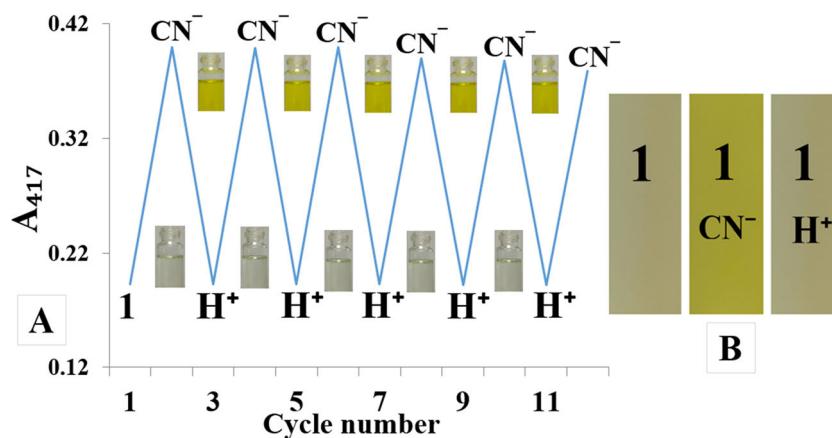
its calculated detection limit is far above the guidelines of WHO (2.0 μM) [6].

Conclusions

The study on optical responses of salophenes **1**–**3** toward CN⁻ showed that hydroxyl groups are playing critical roles in the recognition of this anion. Therefore, probes **1** and **2** are promising CN⁻ indicators in terms of their ease-of-use, highly selectivity, very low detection limit (1–10 nM), visual and emission color change together with rapid response. Moreover, the solution test kits of **1** and **2** for quantitative measurment of CN⁻ was successful. On the other hand, the recognition mechanism of CN⁻ by **1** and **2** is different as evidenced by fluorescence, OH⁻ test, reversibility experiment and ^{1}H NMR measurements. Therefore, probe **1** senses CN⁻ via deprotonation process, whiles **2** recognizes CN⁻ via intramolecular aldimine condensation cyclization, leading to formation of dihydroxyquinoxaline **4**. This distinguished response is related to the specific binding sites of **1** and **2**. Finally, it was found that the calculated detection limits of these probes are significantly superior to those of all reported **S1**-**S13** (Table 1).

Experimental

Materials and Instrumentation

All chemical reagents and solvents were of analytical grade and commercially available. The fluorescence spectra were carried out on a Jasco FP-6500 spectrofluorimeter. The absorbance spectra were recorded on an Agilent 8453 UV-Vis spectrophotometer. Mass spectra were obtained on a Fisons instrument. ^{1}H NMR was measured by Varian 400 MHz. Infrared spectra were recorded on a Perkin Elmer 883 spectrometer.

Fig. 12 Absorbance peaks and colorimetric changes of **1** in 30 % aqueous CH₃CN (**a** and **c**) and **2** in 30 % aqueous MeOH (**b** and **d**) upon addition of various concentrations of CN⁻
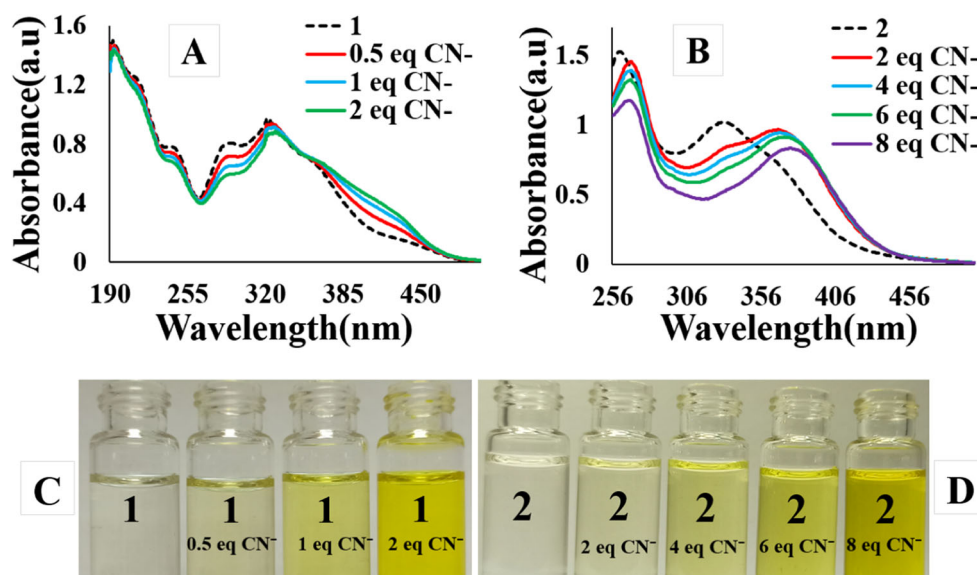
Synthesis of 4

A mixture of compound **2** (1 mmol) and NaCN (8 mmol) in MeOH was stirred at room temperature for 60 min. After removing of MeOH, the solid was extracted with chloroform. The organic layer was dried over sodium sulfate. The orange product **4** was purified by column chromatography and gave 80 % yield.

Dihydroxyquinoxaline **4**: IR (KBr, cm-1): 3400 (O-H), 2921 (C-H), 1610 (C = N), 1470 (C = C), 1226 (C-N); 1 H NMR (DMSO-d6): δ 14.92 (s, 1 H), 10.17 (s, 1 H), 7.44 (d, 1 H), 7.36–7.17 (m, 2 H), 7.06 (t, 1 H), 6.94 (m, 4 H), 6.79 (t, 1 H), 6.63 (m, 3 H), 6.23 (s, 1 H).; MS (EI), m/z (rel. intensity %) 317 (M^+, 100 %), 299 (10 %), 223 (75 %), 196 (60 %).

Fluorescence and UV-vis Titration Measurements of Probes with NaCN

Caution CN^- solutions are also very toxic! All the experiments are strongly recommended to do with respiratory protection under good fume hood. Keep any remaining CN^- solution in alkaline solution of ferrous sulfate (pH > 9).

Receptors **1** or **2** or **4** were dissolved in 100 mL of CH_3CN : H_2O buffered system (7:3, pH 7.4) to make the final concentration of 0.3 μM.

0–100 μL of the NaCN solution (0.5 μM) was transferred to the receptor **1** solution prepared above.

0–300 μL of the NaCN solution (24 μM) was transferred to the receptor **2** solution prepared above.

0–70 μL of the NaCN solution (0.2 μM) was transferred to the receptor **4** solution prepared above.

After mixing the above solutions for a few seconds, Fluorescence and UV-vis spectra of **1** or **2** or **4** were measured at room temperature.

Determination of the Detection Limit

To determine the signal-to-noise ratio (S/N), the absorbance and emission intensities of **1** or **2** or **4** in the presence of NaCN were measured 5 times and the standard deviation of the blank measurements was determined. The measurement of the absorbance was performed in the presence of NaCN ions, and the mean intensity was plotted as a concentration of NaCN to determine the slope. The detection limit (DL) was calculated using the following equation:

$$DL = 3\sigma/m$$

where σ is the standard deviation of the intensity of **1**, **2** and **4** in the presence of NaCN and m is the slope between the intensity (A_0/A) or (I_0/I) and concentration (C_t).

^{1}H NMR of Probes 1, 2 and 4 in the Presence of CN$^-$

Each of compounds **1**, **2** and **4** was added to the NMR tube and then dissolved in DMSO-d_6. Then, 1 equiv. of dissolved NaCN in DMSO-d_6 was added to each solution of receptors. After shaking them for a minute, ^{1}H NMR spectra were measured at room temperature.

Declarations

References

1. Davis F, Higson S (2011) Macrocycles: construction, chemistry and nanotechnology applications. Wiley, Chennai
2. Brnjas-Kraljevi J, Pifat-Mrzljak G (2011) Supramolecular structure and function 10. Springer, Dordrecht
3. Kulig KW (1991) *Cyanide* Toxicity. US. Department of Health and Human Services, Atlanta
4. Young C, Tidwell L, Anderson C (2001) Cyanide: social, industrial and economic aspects. Minerals, Metals and Materials Society, Warrendale
5. Acheampong MA, Meulepas RJW, Lens PNL (2010) Removal of heavy metals and cyanide from gold mine wastewater. J Chem Technol Biotechnol 5:590–611
6. Guidelines for Drinking Water Quality (2008) WHO guidelines values for chemicals that are of health significance in drinking water, 3rd edn. WHO Press, Geneva
7. Xu Z, Chen X, Kim HN, Yoon J (2010) Sensors for the optical detection of cyanide ion. Chem Soc Rev 39:127–137
8. Wang F, Wang L, Chen X, Yoon J (2014) Recent progress in the development of fluorometric and colorimetric chemosensors for detection of cyanide ions. Chem Soc Rev 43:4312–4324
9. Saleem M, Lee KH (2015) Optical sensor: a promising strategy for environmental and biomedical monitoring of ionic species. RSC Adv 5:72150–72287
10. Berhanu AL, Gaurav I, Mohiuddin AK, Malik JS, Aulakh V, Kumar KH, Kim (2019) A review of the applications of Schiff bases as optical chemical sensors. Trends Anal Chem 116:74–91
11. Zhang P, Shi BB, Wei TB, Zhang YM, Lin Q, Yao H, You XM (2013) A naphtholic Schiff base for highly selective sensing of cyanide via different channels in aqueous solution. Dyes Pigm 99: 857–862

12. Li Q, Zhang Jh, Cai Y, Qu Wj, G y. Gao, Lin Q, Yao H, Zhang YM, Wei TB (2015) A facile colorimetric and fluorescent cyanide chemosensor: utilization of the nucleophilic addition induced by resonance-assisted hydrogen bond. Tetrahedron 71:857–862

13. Lee JJ, Lee SY, Bok KH, Kim C (2015) A new dual-channel chemosensor based on chemodosimeter approach for detecting cyanide in aqueous solution: a combination of experimental and theoretical studies. J Fluoresc 25:1449–1459

14. Lee HJ, Park SJ, Sin HJ, Na YJ, Kim C (2015) A selective colorimetric chemosensor with an electron-withdrawing group for multi-analytes CN–and F–. New J Chem 39:3900–3907

15. Leng YL, Zhang JH, Li Q, Zhang YM, Lin Q, Yao H, Wei TB (2016) A highly sensitive colorimetric chemodosimeter for cyanide anion by Michael addition based on a coumarin derivative. New J Chem 40:8607–8613

16. Udhayakumari D, Velmathi S, Boobalan MS (2015) Novel chemosensor for multiple target anions: The detection of F–and CN– ion via different approach. J Fluor Chem 175:180–184

17. Sharma S, Hundal MS, Hundal G (2013) Dual channel chromo/fluorogenic chemosensors for cyanide and fluoride ions – an example of in situ acid catalysis of the Strecker reaction for cyanide ion chemodosimetry. Org Biomol Chem 11:654–661

18. Bhalla V, Pramanik S, Kumar M (2013) Cyanide modulated fluorescent supramolecular assembly of a hexaphenylbenzene derivative for detection of trinitrotoluene at the attogram level. Chem Commun 49:895–897

19. Rezaeian K, Khanmohammadi H, Gholizadeh S, Dogaheh (2018) Studies on a multifunctional chromo-fluorogenic sensor for dual channel recognition of Zn^{2+} and CN^- ions in aqueous media: mimicking multiple molecular logic gates and memory devices. New J Chem 42:2158–2166

20. Ryu KY, Lee JJ, Kim JA, Park DY, Kim C (2016) Colorimetric chemosensor for multiple targets, Cu^{2+}, CN^- and S^{2-}. RSC Adv 6:16586–16597

21. HY, Lee SA, Na YJ, Park GJ, Kim C (2015) A colorimetric Schiff base chemosensor for CN^- by naked-eye in aqueous solution. Inorg Chem Commun 54:73–76

22. Mohammadi A, Jabbari J (2016) Simple naked-eye colorimetric chemosensor based on Schiff-base for selective sensing of cyanide and fluoride ions. Can J Chem 94:631–636

23. Olea-Román D, Bélanger-Desmarais N, Flores-Álamo M, Bazán C, Thouin F, Reber C, Castillo-Blum SE (2015) Spectroscopic studies of lanthanide complexes of varying nuclearity based on a compartmentalised ligand. Dalton Trans 44:17175–17188

24. Joshu L, Benítez H, Jiménez-Cruz P, Cureño-Hernández KE, Solano-Peralta A, Flores-Álamo M, Flores-Parra A, Gracia-Mora I, Castillo-Blum SE (2018) $[V^{IV}O]^{2+}$ complexes: Structure, unusual magnetic properties and cytotoxic effect. Inorg Chim Acta 480:197–206

25. . Mota VZ, de Carvalho GSG, Corbi PP, Bergamini FRG, Formiga ALB, Diniz R, Freitas MCR, Cuin A, da Silva AD (2012) Crystal structure and theoretical studies of the keto-enol isomerism of N,N′-bis(salicylidene)-o-phenylenediamine (salophen). Spectrochim Acta A Mol Biomol Spectrosc 99:110–115

26. Reich BJE, Justice AK, Beckstead BT, Reibenspies JH, Miller SA (2004) Cyanide-Catalyzed Cyclizations via Aldimine Coupling. J Org Chem 69:1357–1359

27. Reich BJE, Greenwald EE, Justice AK, Beckstead BT, Reibenspies JH, North SW, Miller SA (2005) Ene-diamine versus Imine-amine Isomeric Preferences. J Org Chem 70:8409–8416

28. Gorginpour F, Zali-Boeini H, Amiri Rudbari H (2021) A quinoxaline-based porous organic polymer containing copper nanoparticles CuNPs@Q-POP as a robust nanocatalyst toward C–N coupling reaction. RSC Adv 11:3655–3665

29. Darabi HR, Kargar M, Hajipoor R, Abouali N, Aghapoor K, Jadidi K, Notash B, Sayahi H (2016) Synthesis and structure of 2,6-bis(2-methoxyphenyl)dithiazolo[4,5-b:5′,4′-e]pyridine) as a novel fluorescent sensor: different recognition of transition metal ions and proton. Tet Lett 57:256–259

30. Darabi HR, Mirzakhani M, Aghapoor K, Faraji L, Sakhaee N, Jadidi K (2013) A structure-activity relationship study on the Wacker oxidation of stilbenes at ambient condition. J Organomet Chem 740:131–134

31. Kawase T, Tanaka K, Fujiwara, N, Darabi HR, Oda M (2003) Complexation of a carbon nanoring with fullerenes. Angew Chem Int Ed Engl 42:1624-1628

32. Darabi HR, Darestani Farahani A, Karouei MH, Aghapoor K, Firouzi R, Herges R, Mohebbi AR, Naether C (2012) Cup-shaped E,E-Stilbenophane: synthesis, crystal structure and supramolecular chemistry. Supramol Chem 24:653–657

33. Darabi HR, Azimzadeh M, Motamedi A, Firouzi R, Herges R, Mohebbi AR, Nasseri S, Naether C (2009) Synthesis, crystal structure and silver complexation of a novel saddle-shaped stilbenophane: NMR and theoretical study on the complex. Supramol Chem 21:632–837

34. Darabi HR, Sobhani L, Rastgar S, Aghapoor K, Amini SK, Zadmard R, Jadidi K, Notash B (2019) Synthesis, characterization and selective Cu^{2+} recognition of novel E– and Z–stilbenophanes. Supramol Chem 31:45–51

35. Darabi HR, Khatamifar E, Aghapoor K, Sayahi H, Firouzi R (2017) Practical and theoretical aspects of Wacker oxidation of tolanophanes: synthesis and characterization of novel diketonic cyclophanes. Appl Organometal Chem 31:e3812

36. Darabi HR, Mirzakhani M, Aghapoor K (2015) The supramolecular effect of stilbenophanes on the Wacker oxidation progress: a structure-activity relationship study. J Organometal Chem 786:10–13

37. Assadollahnejad N, Kargar M, Darabi HR, Abouali N, Jamshidi S, Sharifi A, Aghapoor K, Sayahi H (2019) A new ratiometric, colorimetric and "turn-on" fluorescent chemosensor for the detection of cyanide ions based on a phenol–bisthiazolopyridine hybrid. New J Chem 43:13001-13009

38. Kargar M, Darabi HR, Sharifi A, Mostashari A (2020) A new chromogenic and fluorescent chemosensor based on a naphthol–bisthiazolopyridine hybrid: a fast response and selective detection of multiple targets, silver, cyanide, sulfide, and hydrogen sulfide ions and gaseous H_2S. Analyst 145:2319–2330

39. Ebadinia L, Darabi HR, Ramazani A (2020) Optical detection of cyanide by palladium(II)-dithiazolopyridine probe at the parts per billion level. Phosphorous Sulfur Silicon 195:620

40. Nazarian R, Darabi HR, Aghapoor K, Firouzi R, Sayahi H (2020) A highly sensitive "ON–OFF" optical sensor for the selective detection of cyanide ions in 100% aqueous solutions based on hydrogen bonding and water assisted aggregation induced emission. Chem Commun 56:8992-8995

41. Kumari N, Jha S, Bhattacharya SJ (2011) Colorimetric probes based on anthraimidazolediones for selective sensing of fluoride and cyanide ion via intramolecular charge transfer. J Org Chem 76:8215–8222

42. Wei TB, Yan GT, Li H, Zhu YR, Shi BB, Lin Q, Yao H, Zhang YM (2016) A highly sensitive and selective "turn-on" fluorescence sensor for rapid detection of cyanide ions in aqueous solution. Supramol Chem 28:720–726

43. Albayrak C, Odabasoglu M, Büyükgüngör O, Lönnecke P (2004) 5-(2-Chlorophenyldiazenyl) salicylaldehyde and 4-(2-chlorophenyldiazenyl)-2-{[tris (hydroxymethyl) methyl] aminomethylene} cyclohexa-3, 5-dien-1 (2H)-one. Acta Crystallogr C60:o318–o320

44. Beer PD, Gale PA (2001) Anion recognition and sensing: the state of the art and future perspectives. Angew Chem Int Ed 40:486-516